Study on Small Fatigue Crack Growth Rate of SLM AlSi10Mg Alloy

Study on Small Fatigue Crack Growth Rate of SLM AlSi10Mg Alloy

Zhen Wang[1], Xuan Ye[2], Xide Li[3] and Xiaoming Liu[1,*]

[1]LNM, Institute of Mechanics, Chinese Academy of Sciences, Beijing 100190
[2]Institute of Nuclear and New Energy Technology, Tsinghua University, Beijing 100084
[3]Department of Engineering Mechanics, Tsinghua University, Beijing, 100084
First author's e-mail: zhenwang@imech.ac.cn
[*]Corresponding author's e-mail: xiaomingliu@imech.ac.cn

Abstract. In this paper, the fatigue small crack growth rate of selective laser melting (SLM) AlSi10Mg alloy is studied by in-situ SEM experiment. The experimental results show that the small crack growth rate of SLM AlSi10Mg alloy can be described by Paris law, and the crack growth rate increases significantly with the increase in temperature. In addition, the combination of finite element simulation and fracture analysis shows that the pore is one of the main factors affecting the dispersion of small crack growth rate.

1. Introduction

Due to its large freedom in structure design and manufacturing, maximum saving of material cost and improvement of production efficiency, additive manufacturing (AM) technology has attracted the wide attention of researchers [1]. As a mature AM technology, SLM technology has been applied to manufacture the structural parts using the AlSi10Mg alloy. The research shows that the tensile mechanical properties of AM alloys are usually better than those of traditional castings [2]. To promote the engineering application of AlSi10Mg alloy, it is necessary to explore the mechanism of its fatigue fracture performance.

In the aspect of fatigue properties, the growth behavior of small cracks has always been a widespread concern of researchers. The main reason is that small cracks are easily affected by inclusions, holes, and grain boundaries due to their small size. Therefore, it is difficult to simply describe the propagation rate of fatigue crack by Paris law because of the large dispersibility. However, in the whole life cycle of metal materials, the growth of small cracks accounts for 80% of the total life [3]. Therefore, it is extremely urgent to accurately characterize the small crack propagation behavior of SLM AlSi10Mg alloy. However, the research on the small crack propagation behavior of SLM AlSi10Mg alloy mainly focuses on long cracks. Giovanni et al. [4] carried out research on the long crack propagation of SLM AlSi10Mg alloy under different manufacturing directions and heat treatment at room temperature. The results show that the growth rate of the long crack is in good agreement with Paris law, and under the same load, the propagation rate of the long crack depends on the laser scanning direction. At the same time, compared with the results of specimens without heat treatment, the crack growth rate of T6 heat treatment is reduced, and the anisotropy degree of the crack growth rate is reduced. However, regarding the propagation behavior of small cracks, other alloys have also been studied, such as AM Ti6Al4V [5], a nickel-based single-crystal superalloy [6]. For the AlSi10Mg alloy, Zhao et al. [7] carried out in-situ tensile at room temperature to observe the crack propagation process, and they observed the phenomenon of microcracks crossing the boundary of the

molten pool, but did not study the fatigue properties. Bao et al. [8] combined with in-situ synchrotron radiation technology, studied the pore structure evolution and fracture characteristics of SLM AlSi10Mg alloy at room temperature and 250°C under ultra-low cycle fatigue. However, they did not discuss the crack growth rate. Accurate evaluation of small crack growth rate is helpful to reliably predict the fatigue life of SLM AlSi10Mg. Therefore, it is necessary to study the small crack growth rate of SLM AlSi10Mg alloy.

In this study, we used an in-situ SEM high-temperature fatigue device to study the small crack propagation behavior of SLM AlSi10Mg alloy. The propagation length of small cracks in different periods is counted, and the amplitude of the stress intensity factor is characterized. Finally, the dispersion of fatigue crack propagation is analyzed by fracture analysis and finite element simulation.

2. Methods and Materials of Experiment

The preparation method of fatigue specimens of AlSi10Mg alloy used in this study has been described in detail in previous studies [9]. The 3D-printed test piece is a dog-bone shape with a U-notch, and its specific size is shown in Figure 1. In this paper, all the experimental specimens are those with a laser scanning speed of 1000 mm/s. We mainly carried out the two test pieces in the in-situ SEM setup, and the temperatures are at room temperature and 400°C, respectively. Stress control is adopted in the experiment. The maximum stress is σ_{max}=160MPa, so the stress ratio is R = 0.2. The loading spectrum is sinusoidal.

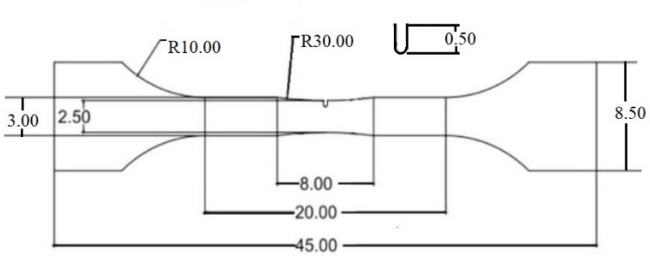

Figure 1. Geometry size of the SLM AlSi10Mg fatigue specimen (unit: mm)

To accurately record the propagation length of the fatigue small crack, the surface of the fatigue test piece was polished until no obvious scratch is observed. Considering that the imaging mode of SEM is scanning imaging mode, it takes 30 seconds to get a clear picture of the surface topography. Therefore, without suspending the experiments, the obtained photos will be severely distorted. To calculate the propagation rate of small cracks, the fatigue machine will be forced to suspend the experiment under specific cycles. The small crack propagation length (a_i) and cycle number (N_i) will be recorded. Therefore, the small crack propagation rate can be calculated based on formula (1). The subscript *i* indicates the cycle of the currently suspended experiment, and *i*-1 indicates the last suspended experiment.

$$\frac{da}{dN} = \frac{a_i - a_{i-1}}{N_i - N_{i-1}} \tag{1}$$

3. Experimental Results and Discussions

3.1. Small Fatigue Crack Propagation Rate

According to the calculation results of formula (1), the curve between the small crack propagation rate and fatigue cycle is shown in Figure 2. It can be seen that for SLM AlSi10Mg alloy, with the increase of fatigue cycles, the growth rate of small cracks increases gradually. However, there are still some rate values with large fluctuations. To explain this phenomenon, we observed the fracture morphology of the small crack growth zone, and the observation results are shown in Figure 2. For the test piece at room temperature, there is a large spherical hole 148.2 μm from the notch, and it is located on the subsurface of the test piece. It denotes Pore 1. In addition, there are some small pores in the center of

the specimen. Similarly, for the test piece at 400 °C, there are two pores in the fracture surface, one at the center of the test piece and the other at the subsurface position. Some studies have shown that the formation of pores in SLM AlSi10Mg alloy is because the AlSi10Mg powder cannot be completely melted and there is not enough liquid phase to fill the voids in the molten pool [10]. Therefore, some pores with the size of tens of micrometers are formed. However, these pores affect the crack growth rate. Pores 1 and 3 exist on the subsurface, which results in an abnormal increase in the crack growth rate. It finds that Pore 2 did not cause a sudden increase in the crack growth rate. This phenomenon will be detailed in Section 3.2.

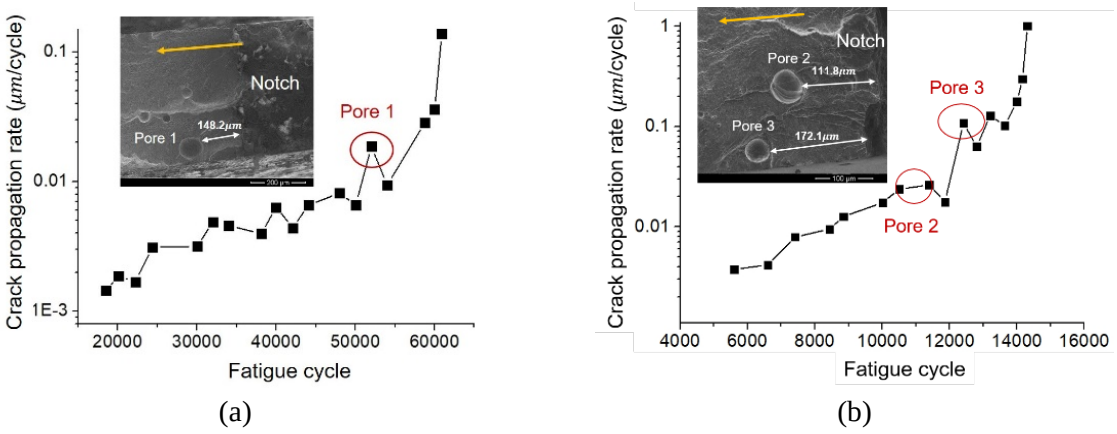

Figure 2. Fatigue small crack propagation rate curve and fracture morphology of SLM AlSi10Mg alloy at (a) room temperature; (b) 400°C

In addition to obtaining the curve of crack growth rate with fatigue cycles, the crack tip driving force is also a concern of researchers. Commonly, it mainly includes stress intensity factor based on linear elastic fracture mechanics [11] and J-integral based on elastic-plastic fracture mechanics [12]. Qian et al. found that the magnitude of the stress intensity factor can characterize a small crack propagation rate for AM Ti6Al4V alloy by using Paris law [5]. Therefore, considering the geometric size of the specimen and the available data, we would also use the amplitude of the stress intensity factor to characterize the crack propagation rate of SLM AlSi10Mg alloy. For a single-side-notch specimen containing a crack, the theoretical expression of stress intensity factor amplitude ΔK during fatigue loading established by Kujawski et al. [13] is applied:

$$\Delta K = 1.122\Delta\sigma\sqrt{\pi l}\,\frac{k_t}{k_t-1}\left[(1+2\frac{a}{r})^{-1/2}+(1+2\frac{a}{r})^{-3/2}\right]\sqrt{\frac{a}{r}}\ , \qquad a \le 0.2r \tag{2-1}$$

$$\Delta K = 1.122\Delta\sigma\sqrt{\pi l}\sqrt{1+\frac{a}{r}(\frac{2}{k_t-1})^2}\ , \qquad a > 0.2r \tag{2-2}$$

In formula (2), k_t is the stress concentration coefficient at the notch of the specimen, l is the notch depth, r is the notch radius, and the stress amplitude is $\Delta\sigma$, and its calculation formula is $\Delta\sigma = \Delta F/[d\times(w-l-a)]$. Where d is the thickness of the specimen. Relationship between stress intensity factor amplitude (ΔK) and crack growth rate (da/dN) is showed in Figure 3.

Therefore, we use the Paris formula (3) to fit the crack growth rate logarithmically by using the least square method. The fitting parameters are shown in Table 1. For the ductile metal materials, the value range of n is 2-4. Our experimental results are satisfactory. To ensure the validity of the linear fitting curve, the correlation coefficient, r, is also listed in Table 1. Our fitting results are greater than the minimum value of the correlation coefficient r_0 [14]. In addition, the value of, r, is greater than 0.8, which indicates that for SLM AlSi10Mg alloy, the small crack propagation rate can be predicted by the logarithmic curve of the Paris formula.

$$\frac{da}{dN} = C(\Delta K)^n \quad (3)$$

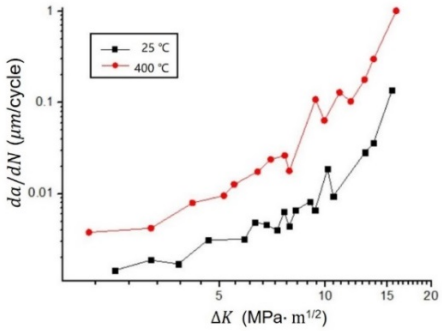

Figure 3. Relationship between stress intensity factor amplitude (ΔK) and crack growth rate (da/dN)

Table 1. Fitting parameters of the Paris formula.

Temperature/°C	25	400
n	2.10	2.71
C	6.82E-10	2.00E-9
Adjusted R-squared/ R^2	0.80	0.88
Minimum value of correlation coefficient [14]	0.47	0.50

3.2. Effect of Microstructure on Small Crack Growth Rate

Usually, the small crack propagation rate is significantly affected by microstructure, such as inclusions, grain boundaries, holes, and so on [15]. Therefore, it may show large dispersion or even decrease with the increase of fatigue cycles [16], which would not describe by the Paris formula. However, the propagation rate of long cracks can be characterized by the Paris formula, which is mainly because the crack length is much larger than the microstructure size. For SLM AlSi10Mg alloy, the small crack propagation also has a good consistency and can be described by the Paris formula, which would be related to its microstructure. The microstructure of the SLM AlSi10Mg alloy is observed, as shown in Figure 4. Its microstructure shows that eutectic Si is clustered and integrated into the Al matrix uniformly, forming a network-like structure. A small amount of Si particles are uniformly distributed in the isolated Al matrix. Therefore, on the micrometer scale, the microstructure of the AM alloy is relatively uniform. However, the microstructure of cast Al-Si alloys consists of coarse needle-like or strip-like eutectic Si (tens of micrometers in size) and Al matrix [17]. Therefore, for some cast alloys, it is difficult to predict the growth rate of small cracks through the Paris formula [16].

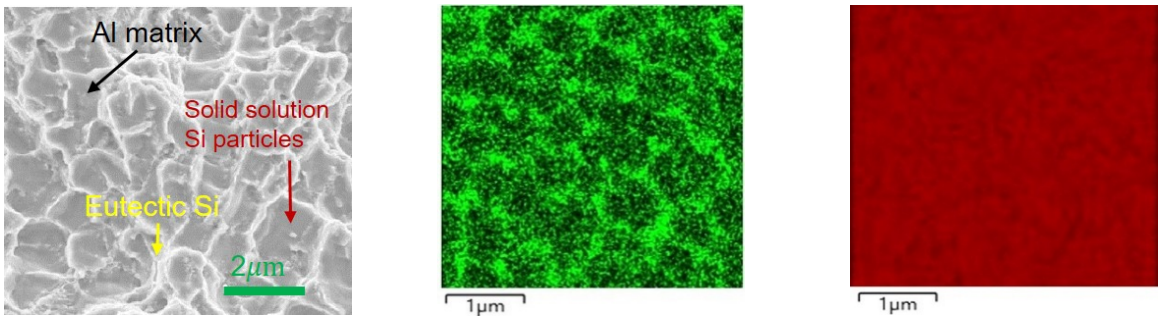

(a) (b) (c)

Figure 4. (a) Microstructure of SLM AlSi10Mg alloy; Composition distribution of (b) Si element; (c) Al element

3.3. Effect of Pore Location on Small Crack Growth Rate

From Section 3.1, we can see that the location of pores has a great influence on the growth rate of small cracks. To explain this phenomenon, we will calculate the influence of the pore location on the stress distribution through the finite element method. As the pore size is much smaller than that of the specimen, the schematic diagram of selecting the representative volume unit of a cube is shown in Figure 5(a), and its side length is 0.5 mm, which is consistent with the thickness of the specimen. By measuring Pore 3 in Figure 2, its diameter is 46.0 μm. In Figure 6, *d* represents the diameter of the spherical pore, and *x* represents the distance from the center of the pore to the surface. To describe the influence of position, it can be depicted by moving the position of the spherical pore in the horizontal direction. The lower edge is a fixed boundary, and the upper edge is subjected to a tensile load with stress of 160MPa. Because the material is polycrystalline and the grains are uniformly distributed, the isotropic model is adopted and element type is C3D10. The stress distribution around pores at different locations is shown in Fig. 6. The stress concentration factor is defined as the ratio of the maximum stress around the hole to the far-field stress. Therefore, the variable curve of the stress concentration factor with pore location is shown in Figure 6.

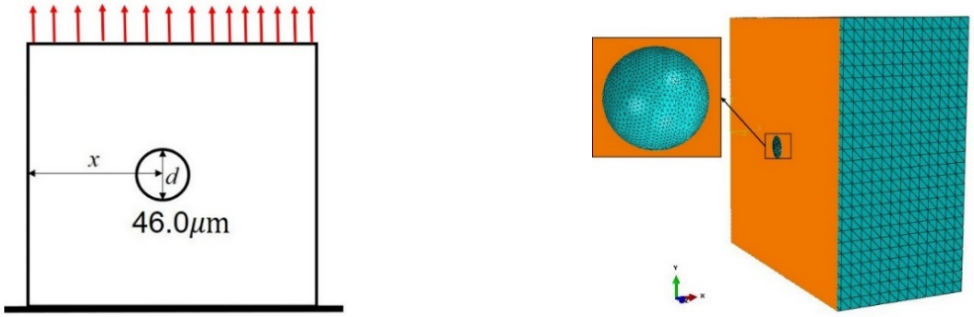

Figure 5. (a) Schematic diagram of representative volume unit; (b) Finite element model

Table 2. Finite element simulation parameters of SLM AlSi10Mg

Elastic parameters		Plastic parameters			
Elastic modulus/MPa	Possion's ratio	Plastic strain/%	0.00	0.40	1.40
76000	0.3	Stress/MPa	280	300	350

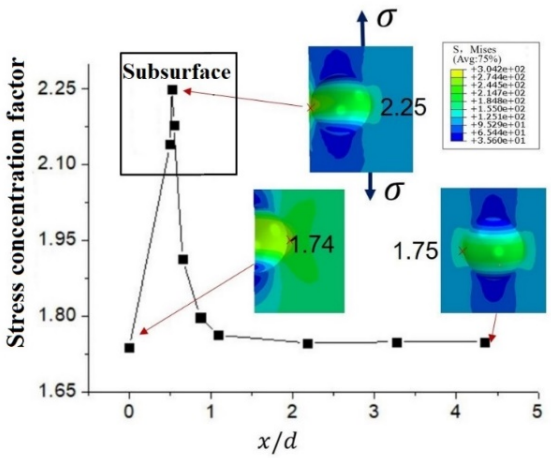

Figure 6. Maximum stress concentration factor around the pore and finite element analysis results

As can be seen from Figure 6, the stress concentration coefficient at the subsurface pore is significantly higher than that at the internal position of the specimen. The large stress concentration coefficient will lead to an increase in stress amplitude in the crack growth process, which will cause the increase of stress intensity factor amplitude around the pore based on the formula (2). According to the Paris formula, the amplitude of the stress intensity factor,ΔK, increases, and the crack growth rate significantly increases.

4. Conclusions

In this paper, based on the high-temperature in-situ SEM fatigue platform, we studied the small crack growth rate of SLM AlSi10Mg alloy at room temperature and 400°C. In addition, the characteristics of small crack growth rates are explained by microstructure observation and finite element analysis. The main conclusions are as follows:

1) For SLM AlSi10Mg alloy, the fatigue small crack growth rate can be described by the Paris formula at room temperature and 400°C. This is mainly due to its uniform distribution of microstructure in the micrometer scale.

2) The pore near the sub-surface has a more significant effect on the growth rate of small cracks, which is mainly due to the significant increase in the stress concentration factor of the pore near the sub-surface.

5. Acknowledgements

This research is supported by the National Natural Science Foundation of China under Grant No. 11632010.

6. References

[1] Kan, W.H., Chiu, L.N.S., Lim, C.V.S. , et al. (2022) A critical review on the effects of process-induced porosity on the mechanical properties of alloys fabricated by laser powder bed fusion. Journal of Material Science, 57, 9818–9865

[2] Qian Y, Bo S, Yusheng S. (2020) Comparative study of performance comparison of AlSi10Mg alloy prepared by selective laser melting and casting. Journal of Material Science Technology, 2020, 41, 199-208.

[3] Ritchie R.O.,(1999) Proceedings of the 7th International Fatigue Congress. Beijing, vol.1 , p3.

[4] Maria T D G, João Teixeira O de M, Giovanni B, Emanuela C, Enrique M C. (2019) Fatigue crack growth behavior of a selective laser melted AlSi10Mg, Engineering Fracture Mechechanic,2019,217:106-564.

[5] Guian Q, Zhimo J, Xiangnan P, Filippo Berto.(2020) In-situ investigation on fatigue behaviors of Ti-6Al-4V manufactured by selective laser melting. International Journal of Fatigue.133.105424

[6] Liang J, Wang Z, Xie, H, Shi, H, Li, X.(2019) In situ scanning electron microscopy analysis of effect of temperature on small fatigue crack growth behavior of nickel-based single-crystal superalloy, International Journal of Fatigue,128, 105195

[7] Lv Z, Juan Guillermo S M, Lipeng D, Hosni I, Aude S (2019) Damage mechanisms in selective laserBmelted AlSi10Mg under as built and different post-treatment conditions. Material Science Engineering A, 764,138-210.

[8] Jianguang B, Shengchuan W, Philip J W, Zhengkai W, Fei L,Yanan F, Wei S. (2020) Defect evolution during high temperature tension-tension fatigue of SLM AISi10Mg alloy by synchrotron tomography. Material Science Engineering A, 792,139-809.

[9] Wang Z, Zhao C, Wang J, Wu W., Li X. (2022) In-situ dwell-fatigue fracture experiment and CPFE simulation of SLM AlSi10Mg alloy at high temperature. International Journal of Fracture, 235(1), 159–178

[10] Yu Kaibin. (2018) Study on Microstructures and Mechanical Properties of A1Si10Mg Alloy Produced by Selective Laser Melting, (Dissertation), South china University of Technology.

[11] Zhang M, Zhang Y, et al. (2019) Judgment criterion of the dominant factor of creep-fatigue crack growth in a nickel-based superalloy at elevated temperature, International Journal of

Fatigue, 118, 176-184.
[12] Almroth P, Sjodin B, Leidermark D, Simonsson K. et. al. (2019) Isothermal and thermomechanical fatigue crack propagation in both virgin and thermally aged Haynes 230, International Journal of Fatigue, 120, 96-106.
[13] Kujawski D. (1991) Estimations of stress intensity factors for small cracks at notches. Fatigue & Fracture of Engineering Material & Structure, 14(10), 953–65.
[14] Shuzhen Xing. (1996) Problems needing attention in linear fitting of test data, Railway construction, 1, 34-35. (in chinese)
[15] Remy L, Alam A, Haddar N, et al. (2007) Growth of small cracks and prediction of lifetime in high-temperature alloys. Material Science and Engineering A, 2007, 40:468–470
[16] Sansoz F, Brethes B, Pineau A. (2001) Propagation of short fatigue cracks from notches in a Ni base superalloy: experiments and modelling. Fatigue & Fracture of Engineering Material & Structure, 25, 41–53.
[17] Ahmed A, El-Hadad S, Reda R, and Dawood O. (2019) Microstructure control in functionally graded Al-Si castings, International Journal of Cast Metals Research,32(2),67-77.